Rakenteiden Mekaniikka (Journal of Structural Mechanics)
Vol. 44, No 2, 2011, pp. 98-112

Case studies of non-linear modelling of metal structures

Mikko Salminen, Markku Heinisuo, Hilkka Ronni and Henri Perttola

Summary. Two case studies of non-linear modelling using the finite element method (FEM) for metal structures both in ambient and in elevated temperatures are presented. The first one deals with shear resistances of thin metal plates involving different initial geometrical imperfections in the analysis. Different eigenmodes are superimposed and their effects on the tension field resistances of rectangular simply supported plates are considered. The plates may be of steel or aluminum. The second case deals with the modelling of bolted steel joints. Many kinds of contact problems and problems due to different buckling modes of steel parts arise when modelling steel members in fire. The paper reviews solutions found in literature. Special attention is devoted to the modelling of the bolts of end plate joints. It is shown that ignoring the effect of the bolt head makes the resistances of the joints very conservative compared to the results yielded by FEM which considers the effects of bolt heads.

Keywords: metal structures, steel joints, effect of imperfections, bolt modelling.

Introduction

Modelling of metal structures at elevated temperatures is of utmost importance when developing new design methods because experiments are extremely expensive to perform. However, experiments should be used to verify numerical results to some extent. Modelling of metal structures at elevated temperatures is a very challenging task due to material non-linearities and large strains which cause geometrical non-linearities. In the case of bolted joints of metal structures that means contact problems. Real structures also have imperfections resulting from fabrication and erection. Due to the above factors, structural analysis must be done with care.

This paper examines some details of the analysis of metal structures based on literature and the experiences of our research team. The authors hope that the presented cases can be of help to those who will be analysing similar cases in the future. The new design rules developed by our team are intended to broaden the present design rules of the most recent European standards for metal structures. The first case deals with the shear resistance of a metal plate when the elevated temperature is not uniform across the plate. The second case deals with problems in defining the resistance and stiffness of bolted end plate joints of metal structures both in ambient and fire conditions. The referred finite element method (FEM) simulations were done using the ABAQUS program. Our research team received the program from CSC – IT Center for Science Ltd.

The best found references are shortly referred to solve the problem as quasi-static in fire. The same applies to citations concerning solutions to contact problems. Finally, some experiments by our research team concerning the modelling of bolt ends are outlined.

Shear resistance of metal plate at non-uniform elevated temperature

Behaviour of a thin metal plate loaded with shear

Let us consider a rectangular simply supported metal plate loaded with pure shear. When the shear force increases from zero, the plate goes through two phases of behaviour, if it is rather thin: Firstly, the plate buckles, and then as the applied force increases, the ultimate load is reached as the tension field yields as shown in Figure 1.

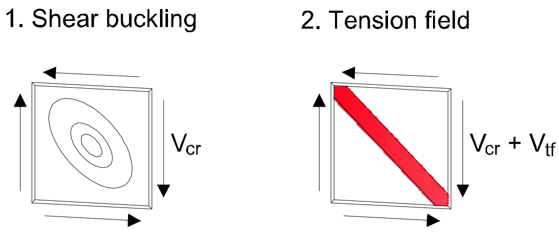

Figure 1. Two phases of thin plate loaded with pure shear as the load increases.

These phases have been observed in tests [1] both in ambient and elevated temperatures. The tests were conducted using welded I-beams which added an extra phase after the yielding of the tension fields: yielding of flanges. The final collapse occurred after this third phase. The design equations for steel plates of the European standard [2] include all these phases, as shown in [3]. The equations of the standard are valid only if the temperature field across the plate is uniform.

Reference [3] also showed how the equations of the standard can be modified to analyse shear buckling when the temperature is not uniform across the plate. All the equations of the standard can be used when the elastic modulus of the plate is reduced by factor $k_{E,\theta}$ at elevated non-uniform temperatures as demonstrated in Figure 2.

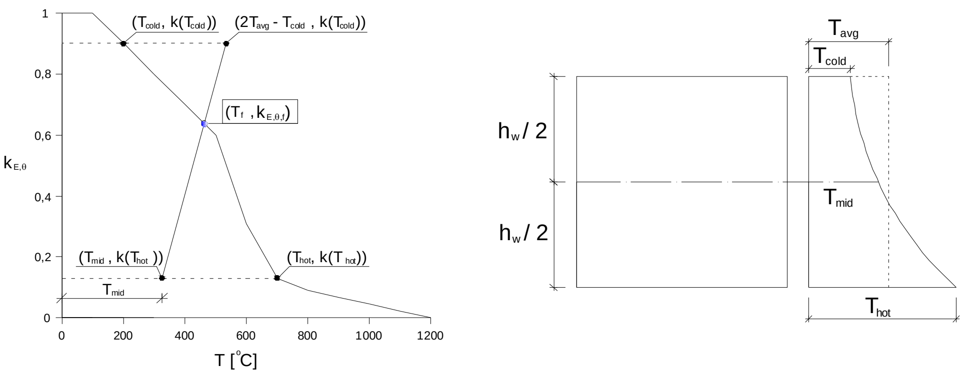

Figure 2. Proposed reduction of elastic modulus for shear buckling [3].

This method was shown to be valid for carbon steel, stainless steel and aluminium – all metal materials for which European standards exist.

Let us consider next the plate in the post-buckling phase when the tension field theory [4] is valid. A similar result has been derived using the so-called “rotated stress field theory” of Standard [5].

FEM analyses of shear resistance

Test results for the beam web at ambient and uniform elevated temperatures (20, 400, 550 and 700 ^{o}C) [1] are used as benchmark cases in FEM simulations. The geometry of the studied simply supported web plate was 305 x 305 x 1.5 mm^3. Uniformly distributed stress of 1 kN/ (t x h) was applied on the edges of the plate. The thickness of the plate was t and its height was h. The stress was multiplied by the load proportionality factor, which gives the maximum shear load of the plate in kN. Perfect elastic-plastic behaviour was used for the steel. Reductions of effective yield strength and elastic modulus at elevated temperatures were done according to EN1993-1-2 Table 3.1 [6]. In further analyses a more accurate material model will be used, because the behavior of steel material is highly nonlinear at elevated temperatures. Each edge of the plate consisted of 50 nodes of four-node reduced-integration quadrilateral shell elements, coded as S4R in ABAQUS. Arc-length control (Riks method) was used as an incrementation procedure. Initial imperfections were needed so that the tension field effect could occur. The three lowest eigenmodes from the linear buckling analysis at ambient temperature were combined so that the maximum magnitude at the midpoint of the plate was h/100 = 3.05 mm as shown in Table 1. The quantity h/100 is the maximum allowed imperfection after the fabrication of the sheet according to Annex D of EN 1090-2 [7].

Table 1. Superimposition of three lowest eigenmodes.

Eigenmode	V_{cr} [kN]	Maximum magnitude [mm]	Magnitude at the midpoint of the plate [mm]	Geometry
1	18.69	2.4132	2.4132	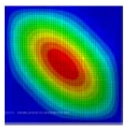
2	23.18	0.7 x h/200 = 1.0675	0	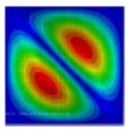
3	50.02	0.7 x 2.4132 = 1.6892	0.6368	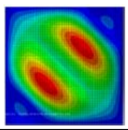

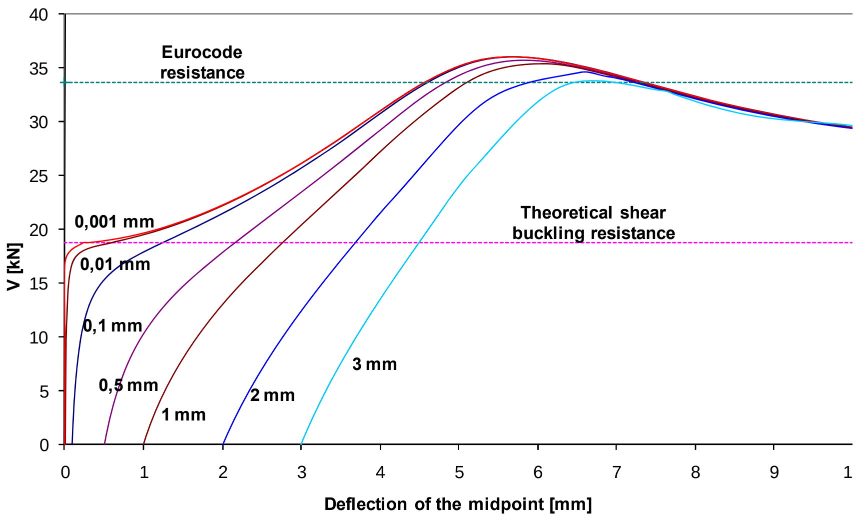

Figure 3. Effect of the magnitude of the lowest eigenmode at ambient temperature.

Ultimate shear resistance is not considerably dependent on the magnitude or the shape of the initial imperfection as shown in Figures 3 and 4. Figure 3 shows the resistances of the benchmark case at ambient temperature when using the first eigenmode with different magnitudes as imperfections.

From Figure 3 it can also be determined that the shear buckling phase is detectable only when the magnitude of the initial imperfection is very small (~ *h*/3000 = 0.1 mm). Figure 4 shows the effect of the shape of the initial imperfection. The four lowest eigenmodes are considered so that the maximum magnitude is 3.05 mm in all cases. Tension field graphs and ultimate shear resistances are shown for all cases.

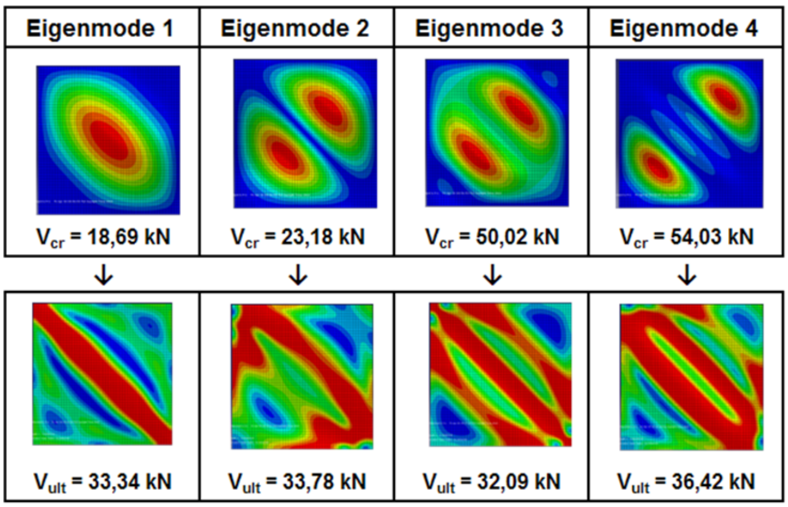

Figure 4. Effect of the shape of the imperfection at ambient temperature.

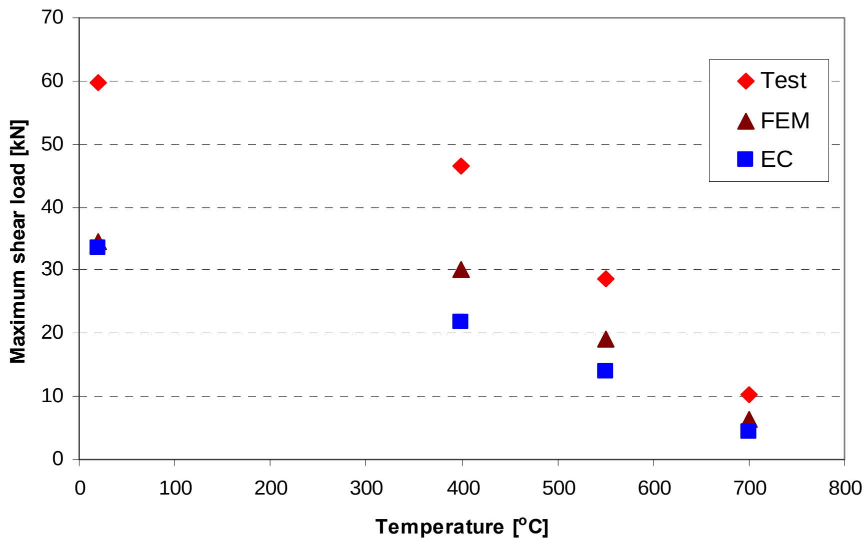

Figure 5. Comparison of shear resistances.

Based on Figure 4, it can be said that ultimate shear resistance does not depend much on the shape of the initial imperfection, especially in the case of the three lowest eigenmodes. However, it should be noted that in some cases (e.g. with a negative eigenmode) the initial imperfection may act as a stiffener and increase the ultimate shear resistance of the plate significantly.

Figure 5 presents the maximum shear loads for the benchmark cases based on Eurocodes [2], [6] and the FEM calculations. Eurocode resistances were calculated for the simply supported plate. Effects of flanges and end-posts were ignored.

Figure 5 indicates that all shear resistances derived from FEM calculations are clearly smaller than resistances from tests, but slightly higher than those derived from Eurocodes. FEM calculations on the above-mentioned plate were extended to non-uniform temperature distributions. Vertical temperature distributions 100-300, 100-500, 100-700, 100-900, 200-500, 300-600, 400-700, 500-800 and 600-900 ^{o}C were considered linear and third degree polynomials so that the hotter temperature was acting on the lower edge of the plate in each case. In the longitudinal direction the temperature was constant.

Calculations at non-uniform elevated temperatures

According to Annex E of EN 1993-1-2 [6], the shear resistance of slender webs at elevated temperatures, $V_{fi,t,Rd}$ is calculated by reducing the shear resistance at ambient temperature, V_{Rd} by the reduction factor of the design yield strength for class 4 cross-sections, $k_{p0,2,\theta}$, which is based on the average temperature of the plate. When partial factors $\gamma_{M0} = \gamma_{M,fi} = 1.00$, $V_{fi,t,Rd}$ is obtained from:

$$V_{fi,t,Rd} = k_{p0,2,\theta,web} V_{Rd} \tag{1}$$

Based on the case described above, preliminary modified EN 1993-1-2 calculation method is proposed for cases where temperature distribution is non-uniform. Compared to the EN 1993-1-2 [6] method, the only difference of this method is that the reduction is based also on the hottest temperature of the plate when $T_{hot} > 500$ °C. The proposed method is presented in Equations (2) – (7) and the factors k_{hot}, k_{cold} and k_{mid}, which take the temperature distribution into account, are presented graphically in Figure 6.

$$V_{fi,t,Rd} = (k_1 k_{p0,2,\theta,web} + (1-k_1) k_{p0,2,\theta,hot}) V_{Rd}, \text{ where} \quad (2)$$

$$k_1 = 1, \text{ when } T_{hot} \leq 500 \text{ °C} \quad (3)$$

$$k_1 = k_{hot} + k_{cold} + k_{mid}, \text{ when } T_{hot} > 500 \text{ °C, where} \quad (4)$$

$$k_{hot} = 1\text{-}0{,}0025(T_{hot} - 500), \qquad 0{,}15 \leq k_{hot} \leq 1 \quad (5)$$

$$k_{cold} = 0{,}0018(T_{cold} - 400), \qquad 0 \leq k_{cold} \leq 0{,}4 \quad (6)$$

$$k_{mid} = 0{,}0003(T_{hot} - T_{mid} - 400), \qquad 0 \leq k_{mid} \leq 0{,}1 \quad (7)$$

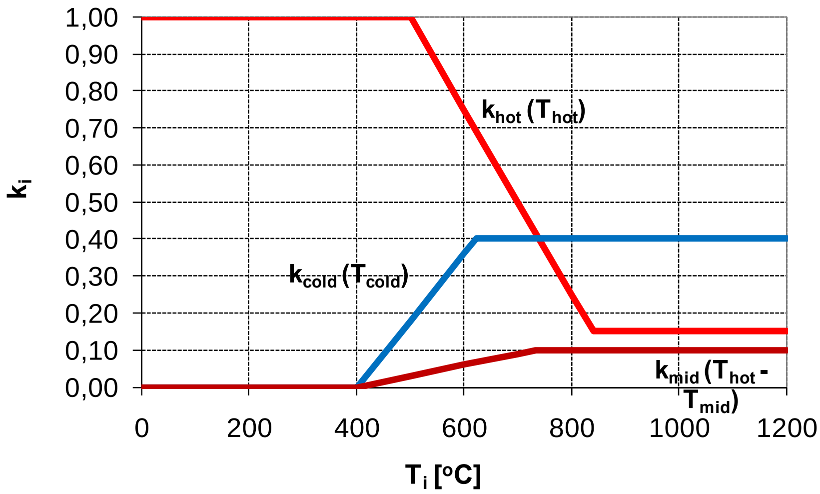

Figure 6. Factors k_{hot}, k_{cold} and k_{mid} of the proposed method.

Based on Equations (2) – (7) and Figure 6, when the hottest temperature of the plate is no more than 500 °C, the reduction for the whole plate can be based on the average temperature. When the hottest temperature of the plate exceeds 840 °C and the coldest temperature is less than 400 °C, the reduction is based mainly (in some cases even 85 %) on the maximum temperature of the plate. Figure 7 shows the yielded regions for four linear temperature distributions when the maximum shear force is acting. It can be seen that when the hottest temperature rises, most of the yielding occurs at the lower part of the web.

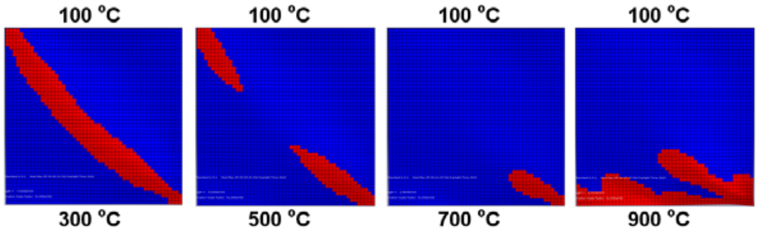

Figure 7. Yielded regions in four cases (linear distributions).

Calculated resistances from FEM and according to EN 1993-1-2 and the proposed method are presented in Tables 2 and 3. Graphical comparisons between FEM and both calculation methods as function of the hottest temperature are shown in Figure 8.

Table 2. Calculated shear resistances [kN] for linear temperature distributions.

	Temperature distribution [°C]								
	100-300	100-500	100-700	100-900	200-500	300-600	400-700	500-800	600-900
FEM	33.69	29.46	13.27	4.61	28.48	19.95	10.53	5.18	3.02
EN 1993-1-2	29.89	26.20	21.83	17.80	24.02	19.82	13.94	7.22	3.36
Proposed method	29.89	26.20	12.76	4.10	24.02	17.30	8.97	4.30	2.54

Table 3. Calculated shear resistances [kN] for non-linear temperature distributions.

	Temperature distribution [°C]								
	100-300	100-500	100-700	100-900	200-500	300-600	400-700	500-800	600-900
FEM	34.59	32.58	20.42	8.29	31.14	23.97	14.74	7.49	3.90
EN 1993-1-2	31.74	29.89	28.05	26.20	27.12	22.92	18.81	12.01	5.79
Proposed method	31.74	29.89	16.63	7.56	27.12	19.58	11.29	6.21	3.80

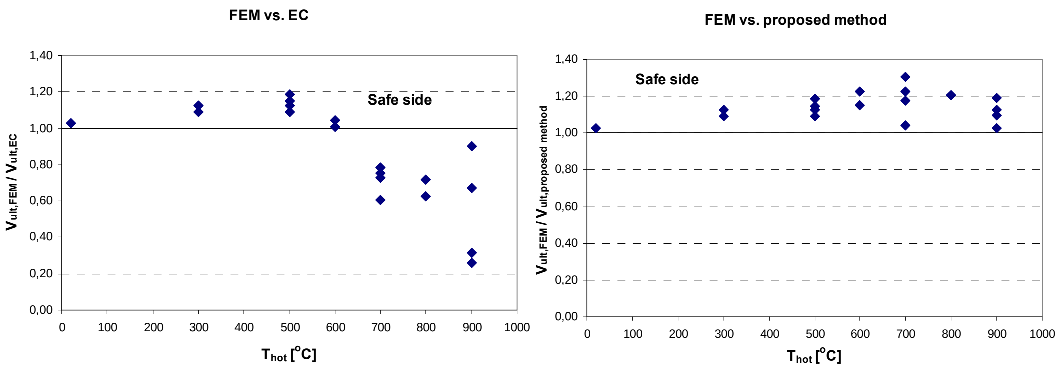

Figure 8. Comparisons of FEM and calculation methods.

Based on Tables 2 and 3 and Figure 8, it can be said that the calculation according to EN 1993-1-2 (using average temperature of the plate) is clearly on the unsafe side in this case, when the hottest temperature of the plate is more than 500 ^{o}C. The proposed method, which takes the temperature distribution into account, gives safe results for all 18 temperature distributions.

FEM modelling of bolted end plate joints of metal structures

General

It may happen that e.g. in the growing phase of a fire some member buckles. As real fires ultimately reach the decay phase, the buckled member may respond again. Such cases are extremely difficult to analyse by static analysis. In fire analysis we often want to analyse structures after some parts of the structures have lost their resistance. References [8] and [9] prove that the use of quasi-static analysis is useful in deriving different failure modes from finite element simulation. Reference [8] uses ABAQUS/Explicit while [9] uses ABAQUS/Standard. In quasi-static analysis a static problem is solved using dynamic equations which add proper damping to the system. If the damping is too strong, some failure modes may go undetected. So, damping should bevery moderate. What, then, is the proper damping factor? It has been shown to be very case dependent, and no clear rules for defining it are found in literature. Figure 9 illustrates the effects of dissipated energy fractions on structural deformations [9]. It shows that when the dissipated energy fraction is too large, the buckling of the beam web cannot be detected in the failure mode.

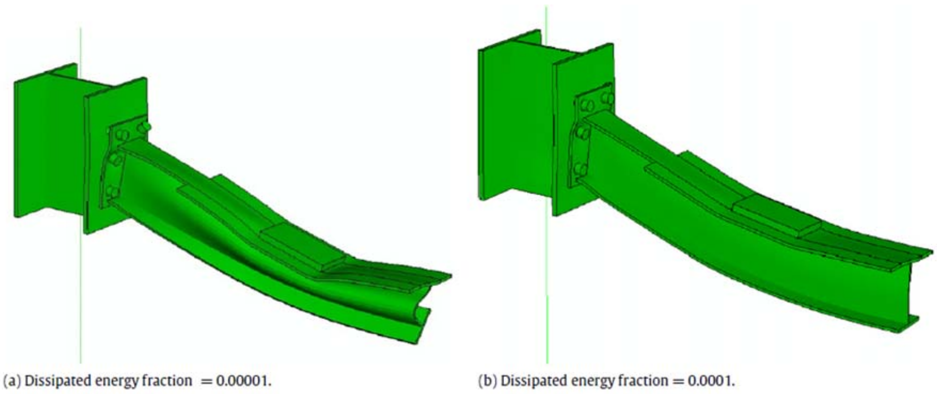

Figure 9. Impact of small and large dissipation fractions [9].

When using a dynamic solution to solve the static problem, the system equation includes two extra terms compared to the static case. Damping was considered above, and the other one is the kinetic energy due to acceleration of the system. Its impact on the final solution must be minor, because it is not present originally. There are at least two ways to check the impact of damping and kinetic energy: by determining the ratio of energy dissipated by damping (parameter ALLSD in ABAQUS) to total strain energy (parameter ALLIE in ABAQUS) or the support reactions of the system. The latter can be used with all programs and is a very “engineer friendly” way of checking the impact. It is proposed [9] that the proper energy ratio ALLSD/ALLIE should be smaller than 0.1 to get reliable results. However, the coarse mesh and improper contact modelling may be the sources of the bad behaviour of the FEM model as regards the bolted joints. The rules for constructing the FEM mesh for bolted end plate joints are given in [8] (see also Fig. 12).

Contact modelling, as well as material and geometrical non-linearities, are the main sources of problems when modelling bolted joints in fire. Contact problems arise

- between bolt shank and hole in end plate and column flange (typically a 2 mm gap),
- between bolt heads, nuts and washers and end plates and column flanges,
- between end plate and column flange.

All these contacts together with possible preloads of the bolts are extremely difficult to model properly. In real structures, there may be some initial gaps between the contact surfaces of the end plate and the column flange due to the fabrication process, and all gaps may not be closed by the preloads of the bolts. Reference [10] gives some rules for modelling the preloads of bolts.

The master-slave algorithm of ABAQUS recognises the surfaces that are in contact and applies constraints (pressure) to slave nodes in order to prevent them penetrating the master surface [10]. The slave part is typically the “weaker” part and the master part the “stronger” part. The frictional effects between surfaces are often included using the classical isotropic Coulomb friction. Friction coefficients between 0-0.3 are reported in literature. The solution is performed incrementally. In the beginning of each increment, an inspection of the state of all contact interactions is performed to determine whether slave nodes are open or closed [10]. If the node is closed, a further check is performed to identify whether the node is sticking or sliding. Constraints are applied by the algorithm to each closed node and released from each open node. This process is repeated until no change is found in the status of all slave nodes. Then, equilibrium iteration is performed, and if the residuals are not within the prescribed tolerance, the increment is neglected and a smaller increment is applied and the procedure is repeated. In some cases the program terminates due to numerical instability before the entire solution can be found. However, all problems have been solved successfully so far through trials and errors.

Base bolt joint

Let us consider the modelling of the bolt end. Actually, the influence of the finite size of the bolt head (or washer) on the response of the end plate joint is considered. In the end plate joint the bolt end (bolt head/nut + washer) is in contact with the end plate and the column flange. To simplify the problem, we can consider the base bolt joint, where this problem affects only the base plate and the bolt head. It is supposed that there are no nuts and washers (calibration nuts) below the base plate of the column. The loading is introduced at the top of the column in such a way that the pure bending alone is present. This can be done by giving a couple at the top of the column and at the same time enforcing the top cross section of a column to remain a plane. So, no shear forces or torsion moment act at the joint which means that contact problems in the horizontal direction need not be considered. The initial data of this problem are the same as in a reference study [11]. The column is HEA200 and the material grade is S355. The base plate is 400x300x10 mm^3 and the measured yield strength 409 MPa. The base bolts are M16 of grade 8.8. The concrete foundation is 1000x1000x600 mm^3 and the concrete grade is C15/20 using Eurocode notations. Figure 10 illustrates the case.

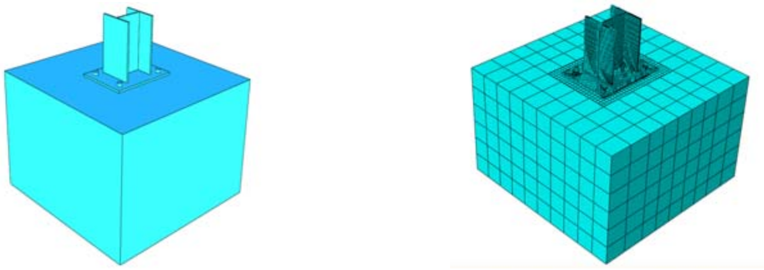

Figure 10. Base bolt joint considered.

Eight-noded linear brick elements C3D8 are used for all parts. An ideal elastic-plastic material model is used as the steel and elastic material model for concrete. The interaction between the contacting parts was defined as a surface-to-surface contact with finite sliding. In normal behaviour, the "hard" pressure-over-closure relationship was required with the appropriate contact constraint enforcement method provided by ABAQUS/Standard. The surfaces in contact could slide freely without friction.

The bolt head was modelled as a steel cylinder 30 mm in diameter completely fixed to the bolt shank. Two millimeter tolerance was modelled symmetrically around the bolt shank meaning a 1 mm gap around the bolt shank. The bolt head bottom surface was fixed to the base plate top surface either by contact options or the TIE parameter of ABAQUS. A tie parameter ties two separate surfaces together so that there is no relative motion between them. The difference between the results yielded by the models was small which is why the final results were calculated using the TIE parameter. Figure 11 shows the results of FEM simulations and experiments for the moment load, moment around the strong axis of the column, and without axial load. The rotations of the joint are calculated from the FEM output using the generalized displacements defined in [12]. These are:

$$
\begin{aligned}
\mathrm{u}_{\mathrm{N}}^{*} &= \frac{1}{A}\int_A u(s)dA \\
\varphi_{\mathrm{y}}^{*} &= \frac{1}{I_z}\int_A u(s)z(s)dA \\
\varphi_{\mathrm{z}}^{*} &= \frac{1}{I_y}\int_A u(s)y(s)dA \\
\varphi^{*} &= \frac{1}{I_\omega}\int_A u(s)\omega(s)dA
\end{aligned}
\qquad (8)
$$

where u(s) are the axial displacements of the member end cross-section from the three dimensional FE calculations, I_z and I_y are the moments of inertia of the cross-section,I_ω is the inertia of the sectorial coordinate of the Vlasov theory,and the integration is done over the cross-section (area A) of the member to be joined at the joint.

In Figure 12 are shown the FEM models of the bolt head and end plate near the bolt. Generalized displacements are calculated at the end cross-section of the member. In standard EN 1993-1-8 the displacements are given at the mid-line of the column in beam to column connection. The motivation of this location to use the generalized displacements is given in [12].

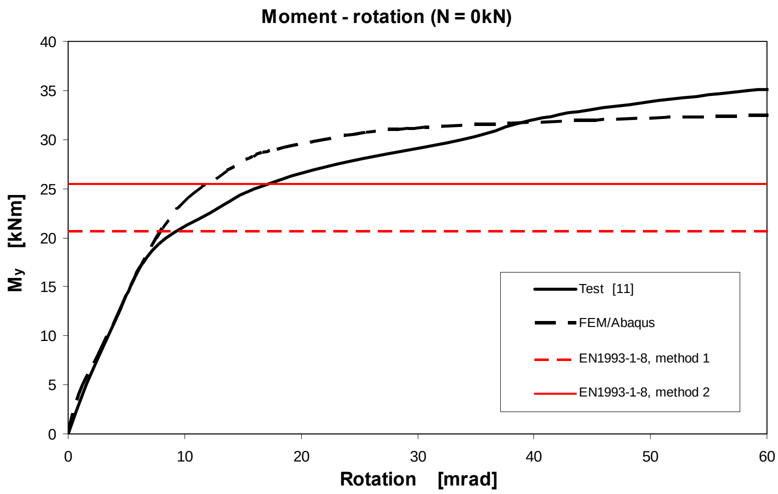

Figure 11. Moment-rotation relationships of the base bolt joint.

Standard [13] also includes method 2 (EN 1993-1-8, Table 6.2), where the influence of the finite size of the bolt head is taken into account on the plastic resistance for type-1 mechanism (yielding of the end plate). This method is based on the doctoral thesis of Jean-Pierre Jaspart [14] and it is described in English, for example, in [17]. The method is based on the assumption that the bolt action is uniformly distributed under the bolt head (or washer or nut). It gives a moment resistance for the joint in question that is about 20% higher than the one estimated by the method 1 (EN 1993-1-8, Table 6.2). The effects of the size of the bolt head were studied in this article using the simplified FEM simulation. The bolt and its hole were replaced by a one-dimensional spring and a solid base plate (no hole) with circular area (diameter D) on the top surface of the base plate. This area correspond the distributing area of the bolt action on the base plate. Furthermore, the kinematic constraint enforcing this round area on the top surface of the base plate to remain a plane is assessed. The diameter of the distributing area was varied from 1.0 mm to 30 mm.

The results of the simulations are shown in Figure 12. It can be seen that the size of the round area is essential for reaching the proper moment resistance for the joint. If the diameter of the distributing area approaches the limiting value of zero, the bolt acts on base plate as a point load causing the occurrence of singularity. Naturally, this kind of modelling does not work properly. With the small values of the diameter, for example, with D = 1 mm, very poor prediction of the response of the joint can be achieved, too. When the diameter of the round is enlarged, the better results can be attained. With the diameter of 30 mm which corresponds the real size of the washer, quite good accuracy is observed when compared the response predicted by this simplified simulation with the full three-dimensional model by continuum elements for all parts of the joint. However, if the disk diameter is smaller than the real nut and washer diameter, the result is on the safe side. In summary, to simulate the actual behaviour of the end plate joint, the full tree-dimensional models are recommended. The same conclusion holds, naturally, both in ambient and fire conditions.

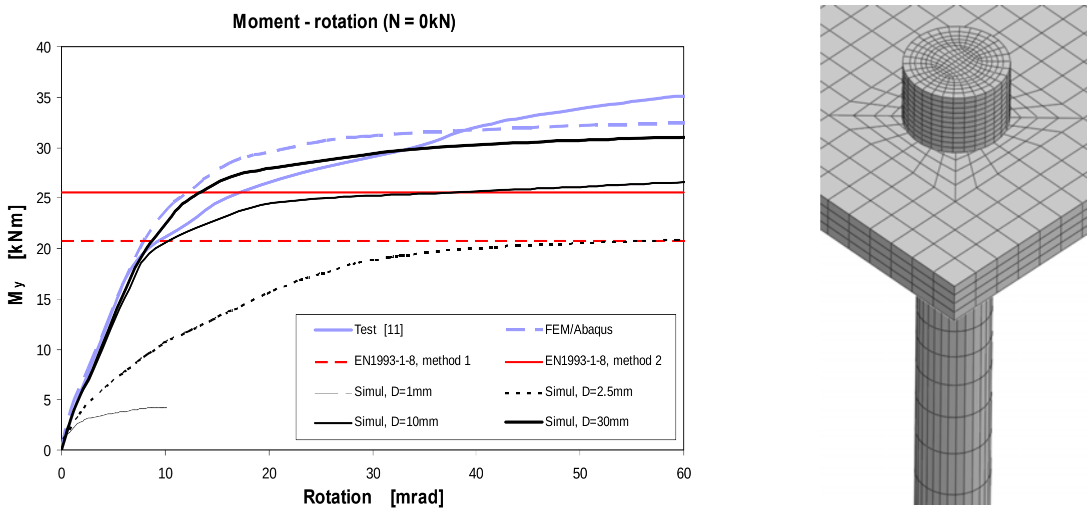

Figure 12. Moment-rotation relationships of the base bolt joint with different bolt end simulations and element mesh for the bolt and the base plate in full 3D model.

Similar results has been obtained for the beam to column joint in [15] and [16]. If the bolt was modelled as a simple one dimensional spring, the moment resistance was much smaller than using the full three dimensional model with continuum elements. Figure 13 illustrates the moment-rotation behaviour of the extended beam end plate joint if the moment load is around the weak axis of the beam. In the analysis with FEA-program Safir, the base plate is discretized by shell elements and bolts are described by one-dimensional beam elements. They are attached to each other at a single nodal point. Then the parametric study with simplified Abaqus model where the springs with distribution areas (as variable) replace the bolts described above have been done again. By changing the diameter D of the distribution are the same response as predicted by Safir-model can be finally achieved. Thus, to simulate the actual behaviour of end plate joints, the full tree-dimensional models are recommended.

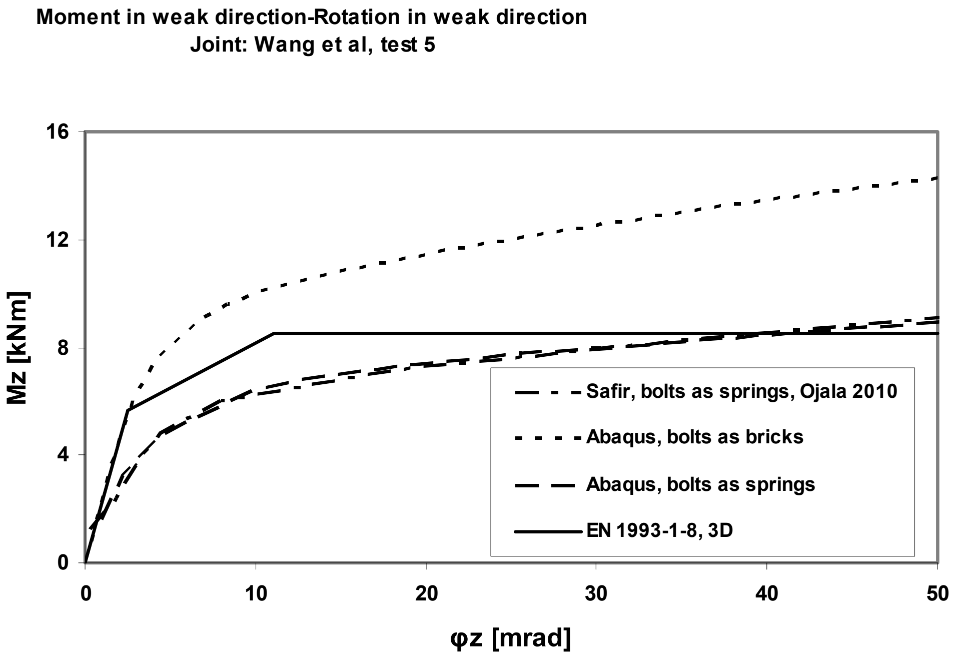

Figure 13. Moment-rotation relationships of the end plate joint with moment around weak axis.

Conclusions

The following conclusions can be drawn based on the case studies of the paper:

- Eurocode rules can be used to define the shear resistance of steel plates at non-uniform elevated temperatures if the maximum temperature is lower than 500 ^{o}C. If the maximum temperature is higher, the reduction proposed in this paper should be used for the range covered in this paper.
- When using the quasi-static solution for the static case, the dissipation fraction should be defined case by case. Support reactions should be checked in these cases.
- Meshing rules for different joint cases can be found in the referred papers. The best found references are presented.
- Contact problems should be formulated with care when considering metal joints. The referred papers include clear rules for end plate joints. The best found references are presented.
- Moment transfer between the bolt head or the nut and the end plate should be taken into account when modelling end plate joints. If that connection is supposed to act as a hinge, the resistance of the joint will be very conservative.

Acknowledgements

The assistance of Mr. Reijo Lindgren from CSC - IT Center for Science Ltd, in constructing the ABAQUS models for this study is gratefully acknowledged.

References

[1] Vimonsatit V., Tan K.H., Ting S.K., *Shear strength of plate girder web panel at elevated temperature*, Journal of Constructional Steel Research 63, 2007, pp. 1442-1451.

[2] EN 1993-1-5, Eurocode 3: *Design of steel structures*, Part 1-5: Plated structural elements, CEN, Bryssels, 2005.

[3] Salminen M., *Shear buckling resistance of thin metal plate at non-uniform elevated temperatures*, Thesis of Licenciate of Science in Technology, Tampere University of Technology, Tampere, 2010.

[4] Dubas P., Gehri E., (Eds.) *Behaviour and Design of Steel Plated Structures*, ECCS Technical Committee 8, Structural Stability, no 44, 1986.

[5] Johansson B., Maqui R., Sedlacek G., *New design rules for plated structures in Eurocode 3*, Journal of Constructional Steel Research 57, 2001, pp. 279-311.

[6] EN 1993-1-2, Eurocode 3: *Design of steel structures*, Part 1-2: Structural fire design, CEN, Bryssels, 2005.

[7] EN 1090-2, *Execution of steel structures and aluminium structures – Part 2: Technical requirements for the execution of steel structures*, CEN, Brussels, 2005.

[8] Yu H., Burgess I., Davison J., Plank R., *Numerical simulation of bolted steel connections in fire using explicit dynamic analysis*, Journal of Constructional Steel Research 64, 2008, pp. 515-525.

[9] Dai X., Wang Y., Bailey C., *Numerical modelling of structural fire behaviour of restrained steel beam-column assemblies using typical joint types*, Engineering Structures 32, 2010, pp. 2337-2351.

[10] Salih E., Gardner L., Nethercot D., *Numerical investigation of net section failure in stainless steel bolted connections*, Journal of Constructional Steel Research 66, 2010, pp. 1455-1466.

[11] Laplume D., Lamblin D., Guerlemnt G., *Computer modeling and experimental base plate column connection used in piping industry*. Fifth International Conference on Computational Structures Technology, Computational Steel Structures Technology, 2000, pp 70-86.

[12] Perttola H., Heinisuo M., *3D component method for base bolt joint*, Paper no 76 in: Proceedings of International Symposium “Steel Structures: Culture & Sustainability 2010”, 21-23 September 2010, Istanbul (accepted paper).

[13] EN 1993-1-8, Eurocode 3: *Design of steel structures*, Part 1-8: Design of joints, CEN, Bryssels, 2005.

[14] Jaspart J., Etude *de la semi-rigidité des neuds poutre-colonne et son influence sur la resistence des ossatures en acier*. PhD Thesis, (in French), Department MSM, University of Liège, Belgium 1991

[15] Ojala A., *Modeling of extended endplate connection in ambient temperatures and fire*, Diploma thesis, Tampere University of Technology, 2010.

[16] Heinisuo M., Laasonen M., Anttila T., Ronni H., *Integration of joint design of steel structures using product model*, 323-324. The International Conference on Computing in Civil and Building Engineering Nottingham, UK 2010
[17] Girão Coelho A. M., Characterization of the ductility of bolted end plate beam-to-column steel connections. PhD Thesis, (in English), University of Coimbra, Portugal, 2004 (in pages 54-56).

Mikko Salminen, Markku Heinisuo, Hilkka Ronni and Henri Perttola
Research Centre of Metal Structures, Tampere University of Technology
Kampusranta 9 C
60320 Seinäjoki
Finland
mikko.a.salminen@tut.fi